Supplementary Materials for

Senescent immune cells accumulation promotes brown adipose tissue dysfunction during aging

Xu Feng, Li-Wen Wang, Ruo-Yu Zhou, Rui Zhou, Lin-Yun Chen, Hui Peng, Yan Huang, Qi Guo, Xiang-Hang Luo, Hai-Yan Zhou

Address all correspondence and request for reprints to:

Prof. Haiyan Zhou E-mail: hyzhou02@csu.edu.cn

The PDF file includes:

Supplementary Figure 1 S100A8^{+} immune cells accumulate in the BAT of aged rats and mice

Supplementary Figure 2 Senescent S100A8^{+} immune cells infiltrated various tissues
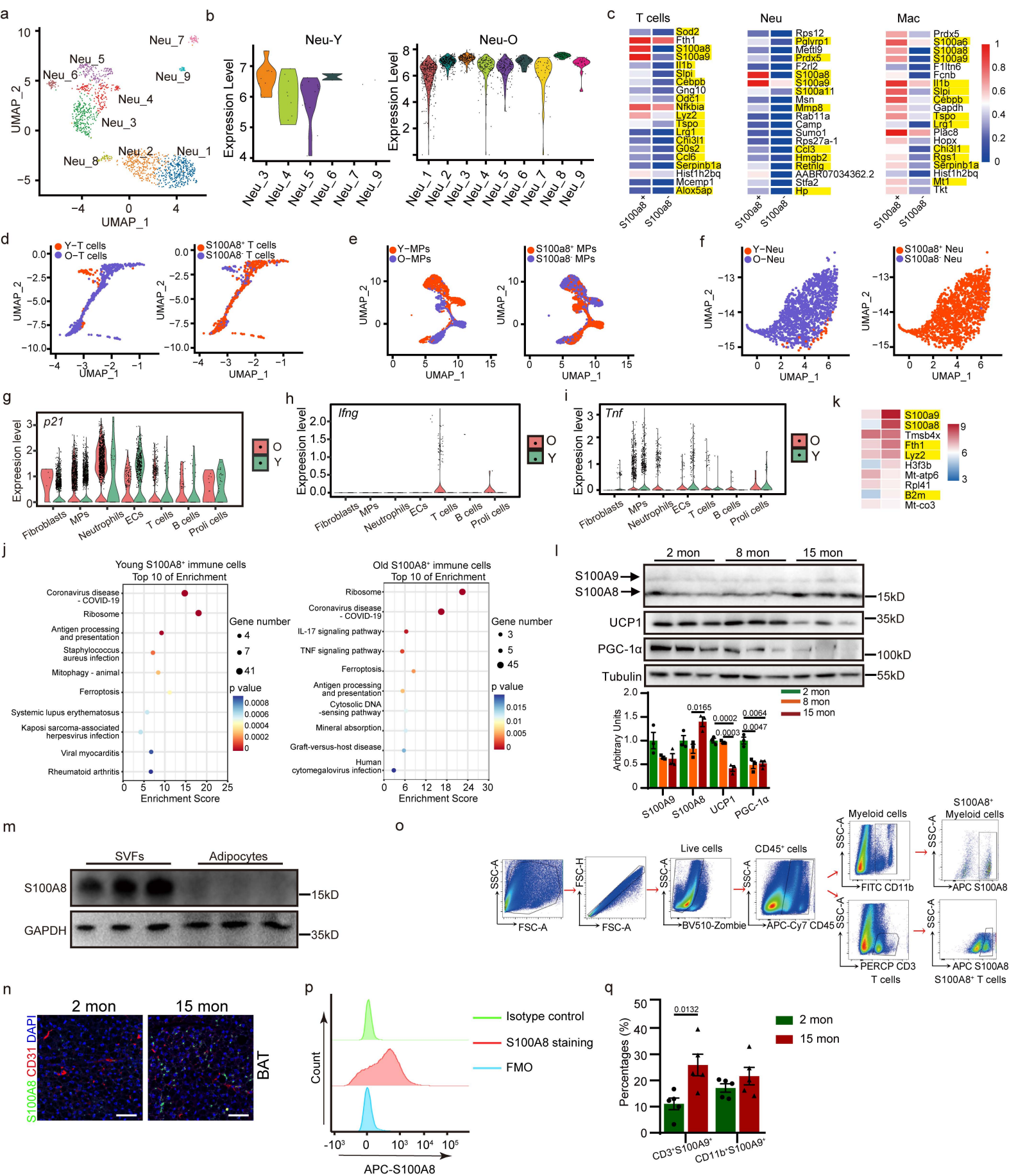
Supplementary Figure 3 Transfer of S100A8^{+} immune cells has no effects on food intake or activity

Supplementary Figure 4 S100A8 inhibits BAT thermogenic function in a way dependent of adipocyte-specific TLR4

Supplementary Figure 5 RBM3 expression in the brown adipocytes is suppressed by S100A8 via TLR4-p38 axis

Supplementary Figure 6 Adipose RBM3 is critical for BAT thermogenic function

Supplementary Table1 Primer sequences used for real time PCR

Supplementary Figure 1

Supplementary Figure 1 S100A8$^+$ immune cells accumulate in the BAT of aged rats and mice

(a) UMAP plot shows clustering of neutrophils based on gene expression.

(b) Violin plots for gene expression of *S100a8* in subclusters of neutrophils in young (5-month-old) and aged (27-month-old) rats.

(c) The 20 most upregulated genes of T cells, neutrophils and macrophages in the BAT of aged rats.

(d-f) Bioinformatics analysis of S100A8$^+$ and S100A8$^-$ cell populations of T cells (d), monocyte-macrophages(e) and neutrophils (f) in the BAT of young and aged rats.

(g-i) Violin plots for gene expression of *p21* (g), *Ifng* (h), *Tnfa* (i) in cell populations of the BAT from young and aged rats.

(j) KEGG analysis of the top 100 genes in S100A8$^+$ immune cells from young (5-month-old) and aged rat (27-month-old), respectively.

(k) Heat-map of the top 10 gene in S100A8$^+$ immune cells from young (5-month-old) and aged rat (27-month-old), respectively.

(l) Representative immunoblots of S100A8 and S100A9 expression in the BAT of 2-, 8-, and 15-month-old mice (n = 3).

(m) Representative immunoblots of S100A8 in the stromal vascular fractions (SVFs) and adipocytes isolated from BAT of 15-month-old mice.

(n) Representative images of S100A8 and CD31 staining in the BAT of 2-month and 15-month-old mice. Scale bar, 50 μm.

(o) Gating strategy of S100A8$^+$ myeloid cells and S100A8$^+$ T cells in the SVFs.

(p) Representative flow cytometry plots for SVFs of BAT stained with S100A8 antibody, isotype IgG antibody control and fluorescence minus one (FMO) control.

(q) Quantification of the frequencies of S100A9$^+$ cells in CD45$^+$ CD3$^+$ T cells and CD45$^+$ CD11b$^+$ myeloid cells in the BAT of 2-, 15-month-old mice (n = 5).

Data shown are representative of three independent experiments with similar results. (n) indicates the number of biologically independent samples examined. Data are shown as the mean ± SEM. Statistical analysis was performed by one-way ANOVA with Bonferroni's multiple-comparisons test (j), or unpaired two-tailed Student's *t*-test (o). Statistical differences were supposed to be significant when $p < 0.05$. Source data are provided as a Source Data File.
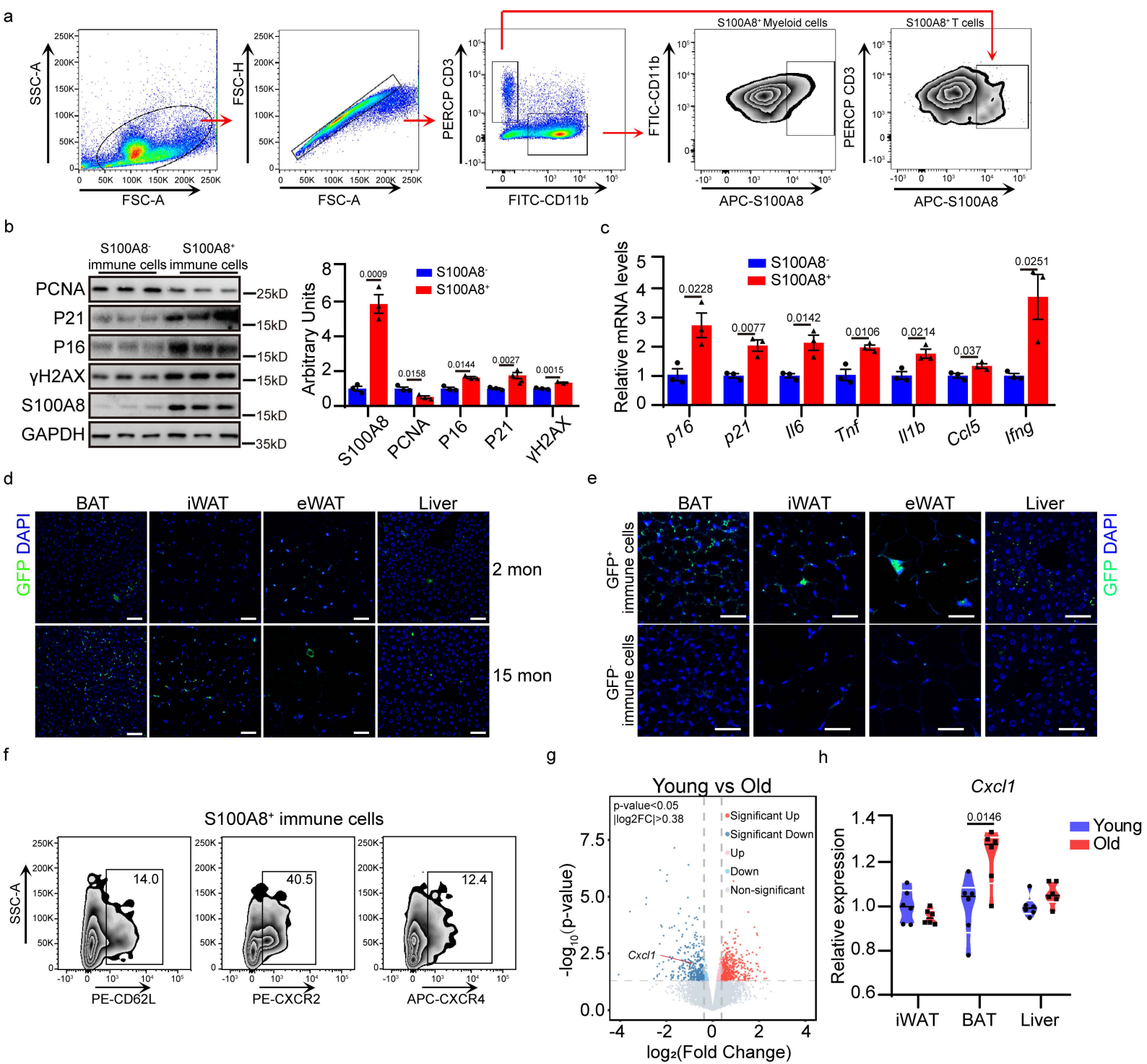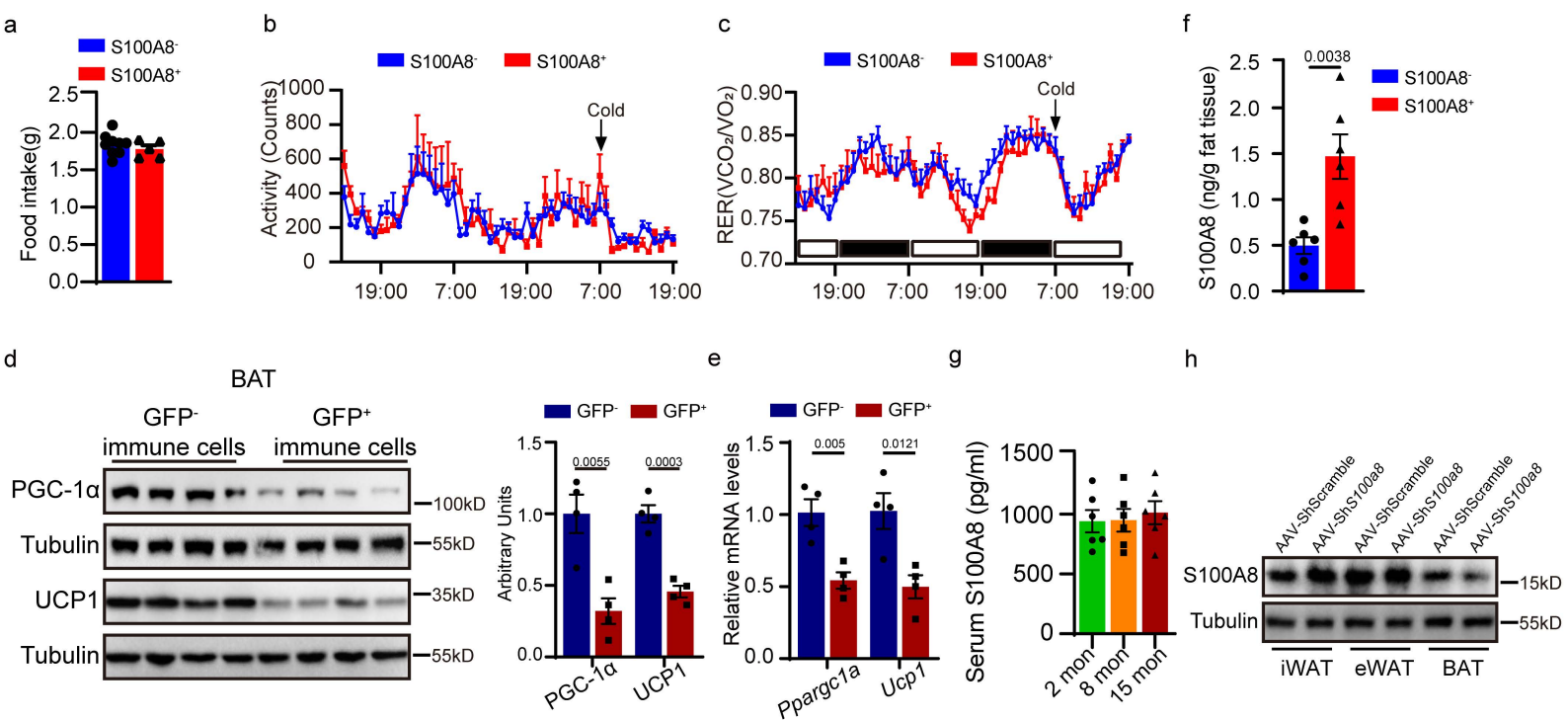
Supplementary Figure 2 Senescent S100A8+ immune cells infiltrate various tissues

(a) Gating strategy of bone marrow S100A8+ myeloid cells and T cells.

(b) Representative immunoblots of PCNA, P21, P16, γH2AX and S100A8 in S100A8- immune cells and S100A8+ immune cells sorted from bone marrow of 15-month-old WT mice (n = 3).

(c) Relative mRNA levels of *p16*, *p21*, *Tnf* and *Ifng* in S100A8- immune cells and S100A8+ immune cells sorted from bone marrow of 15-month-old WT mice (n = 3).

(d) Representative images of GFP staining in BAT, iWAT, eWAT and liver of young (2-month-old) and aged (15-month-old) *S100A8-Cre-EGFP* mice. Scale bar, 50 μm.

(e) Representative images of GFP staining in BAT, iWAT, eWAT and liver of mice transferred with GFP+ immune cells or GFP- immune cells (n=4). Scale bar, 50 μm.

(f) Representative flow cytometry plots for CD62L, CXCR2 and CXCR4 in S100A8+ and S100A8- immune cells.

(g) Volcano plots for differentially expressed genes in BAT of young (5-month-old) mice versus aged (24-month-old) mice (GSE25324).

(h) Violin plots for relative expression of *Cxcl1* in iWAT, BAT and liver in young and aged mice (GSE25324; Black lines indicate median and white lines indicate quartiles).

Data shown are representative of three independent experiments with similar results.　(n) indicates the number of biologically independent samples examined. Data are shown as the mean ± SEM. Statistical analysis was performed by unpaired two-tailed Student's *t*-test (b, c, h). Statistical differences were supposed to be significant when p ＜ 0.05. Source data are provided as a Source Data File.

a

Food intake(g)

S100A8⁻ ■ S100A8⁺

b

Activity (Counts)

S100A8⁻ ■ S100A8⁺

Cold

19:00 7:00 19:00 7:00 19:00

c

RER(VCO₂/VO₂)

S100A8⁻ ■ S100A8⁺

Cold

19:00 7:00 19:00 7:00 19:00

f

S100A8 (ng/g fat tissue)

0.0038

S100A8⁻ ■ S100A8⁺

d

BAT

GFP⁻ immune cells   GFP⁺ immune cells

PGC-1α —100kD
Tubulin —55kD
UCP1 —35kD
Tubulin —55kD

Arbitrary Units

GFP⁻ ■ GFP⁺

0.0055   0.0003

PGC-1α   UCP1

e

Relative mRNA levels

GFP⁻ ■ GFP⁺

0.005   0.0121

Ppargc1a   Ucp1

g

Serum S100A8 (pg/ml)

2 mon   8 mon   15 mon

h

AAV-ShScramble AAV-ShS100a8 AAV-ShScramble AAV-ShS100a8 AAV-ShScramble AAV-ShS100a8

S100A8 —15kD
Tubulin —55kD

iWAT   eWAT   BAT

Supplementary Figure 3

Supplementary Figure 3 Transfer of S100A8$^+$ immune cells has no effects on food intake or activity

(a) Daily food intake of mice transferred with bone marrow S100A8$^-$ or S100A8$^+$ immune cells (n = 5-9).

(b) Activity of mice transferred with bone marrow S100A8$^-$ or S100A8$^+$ immune cells (n = 5-9).

(c) Respiratory exchange rate (RER) of mice transferred with S100A8$^-$ or S100A8$^+$ immune cells (n = 5-9).

(d) Representative immunoblots of UCP1 and PGC-1α of BAT from mice transferred with GFP$^+$ immune cells or GFP$^-$ immune cells (n = 4).

(e) Relative mRNA levels of *Ucp1* and *Ppargc1a* in BAT from mice transferred with GFP$^+$ immune cells or GFP$^-$ immune cells (n = 4).

(f) Measurement of S100A8 protein levels in the BAT of mice transferred with S100A8$^+$ immune cells or S100A8$^-$ immune cells (n = 6).

(g) Serum S100A8 levels of 2-, 8-, and 15-month-old mice (n = 6).

(h) Representative immunoblots showing BAT-specific knockdown of S100a8 expression.

Data shown are representative of three independent experiments with similar results.   (n) indicates the number of biologically independent samples examined. Data are shown as the mean ± SEM. Statistical analysis was performed by one-way ANOVA with Bonferroni's multiple-comparisons test (g) unpaired two-tailed Student's *t*-test (a, d, e, f). Statistical differences were supposed to be significant when $p < 0.05$. Source data are provided as a Source Data File.
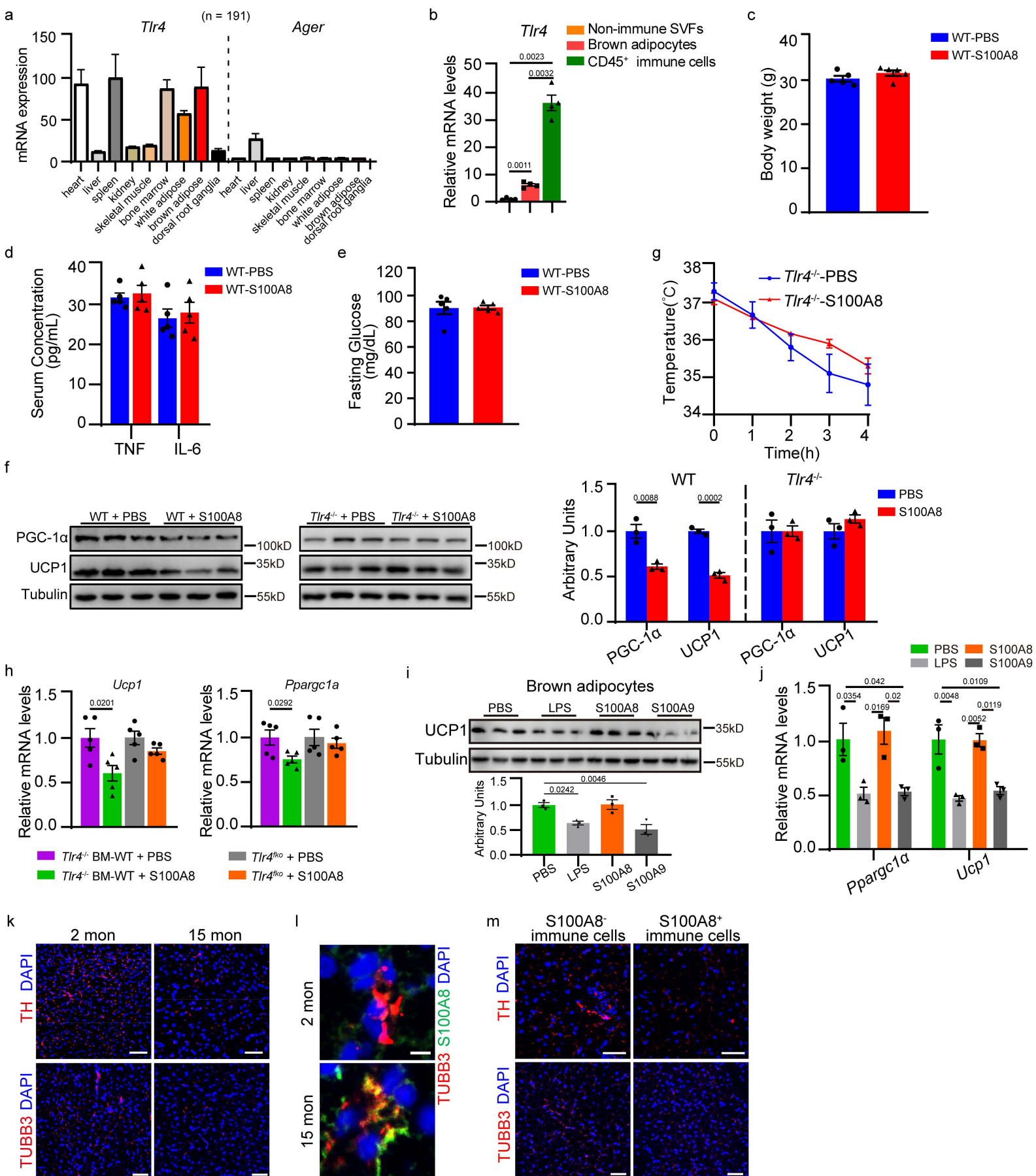
Supplementary Figure 4 S100A8 inhibits BAT thermogenic function in a way dependent of adipocyte-specific TLR4

(a) The expression of *Tlr4* (left) and *Ager* (right) in different tissues was analyzed by the BioGPS database (n = 191).

(b) Expression of *Tlr4* in brown adipocytes, non-immune SVFs, and CD45^{+} immune cells (n = 4).

(c) Body weight of WT mice treated with PBS or S100A8 protein (n = 5).

(d) Serum concentration of TNF-α and IL-6 in WT mice treated with PBS or S100A8 protein (n = 5).

(e) Fasting glucose of WT mice treated with PBS or S100A8 protein (n = 5).

(f) Representative immunoblots of PGC-1α and UCP1 in the BAT of WT and *Tlr4*^{-/-} mice treated with S100A8 (n = 3).

(g) Core body temperature of *Tlr4*^{-/-} mice treated with PBS or S100A8 under cold stimulation (n = 3).

(h) Relative mRNA levels of *Ucp1* and *Ppargc1a* in the BAT of bone marrow

reconstitution mice (*Tlr4*^{-/-}BM-WT) and adipocyte-specific *Tlr4* knockout mice

(*Tlr4*[fko]) with or without S100A8 treatment (n = 5).

(i) Representative immunoblots of UCP1 in brown adipocytes treated with PBS, LPS, S100A8 protein or S100A9 protein (n = 3).

(j) Relative mRNA levels of *Ppargc1a* and *Ucp1* in brown adipocytes treated with PBS, LPS, S100A8 protein or S100A9 protein (n = 3).

(k) Representative images of TH and TUBB3 staining in the BAT of 2-month- and 15-month-old mice. Scale bar, 50 μm.

(l) Representative images of age-associated changes in S100A8 and TUBB3 in the BAT of 2-month-old and 15-month-old mice. Scale bar, 10 μm.

(m) Representative images of TH and TUBB3 staining in the BAT of mice transferred with S100A8^{+} immune cells or S100A8^{-} immune cells. Scale bar, 50 μm.

Data shown are representative of three independent experiments with similar results.　(n) indicates the number of biologically independent samples examined. Data are shown as the mean ± SEM. Statistical analysis was performed by one-way (b, i, j) or two-way ANOVA with Bonferroni's multiple-comparisons test (g), or unpaired two-tailed Student's *t*-test (c, d, e, f, h). Statistical differences were supposed to be significant when $p < 0.05$. Source data are provided as a Source Data File.
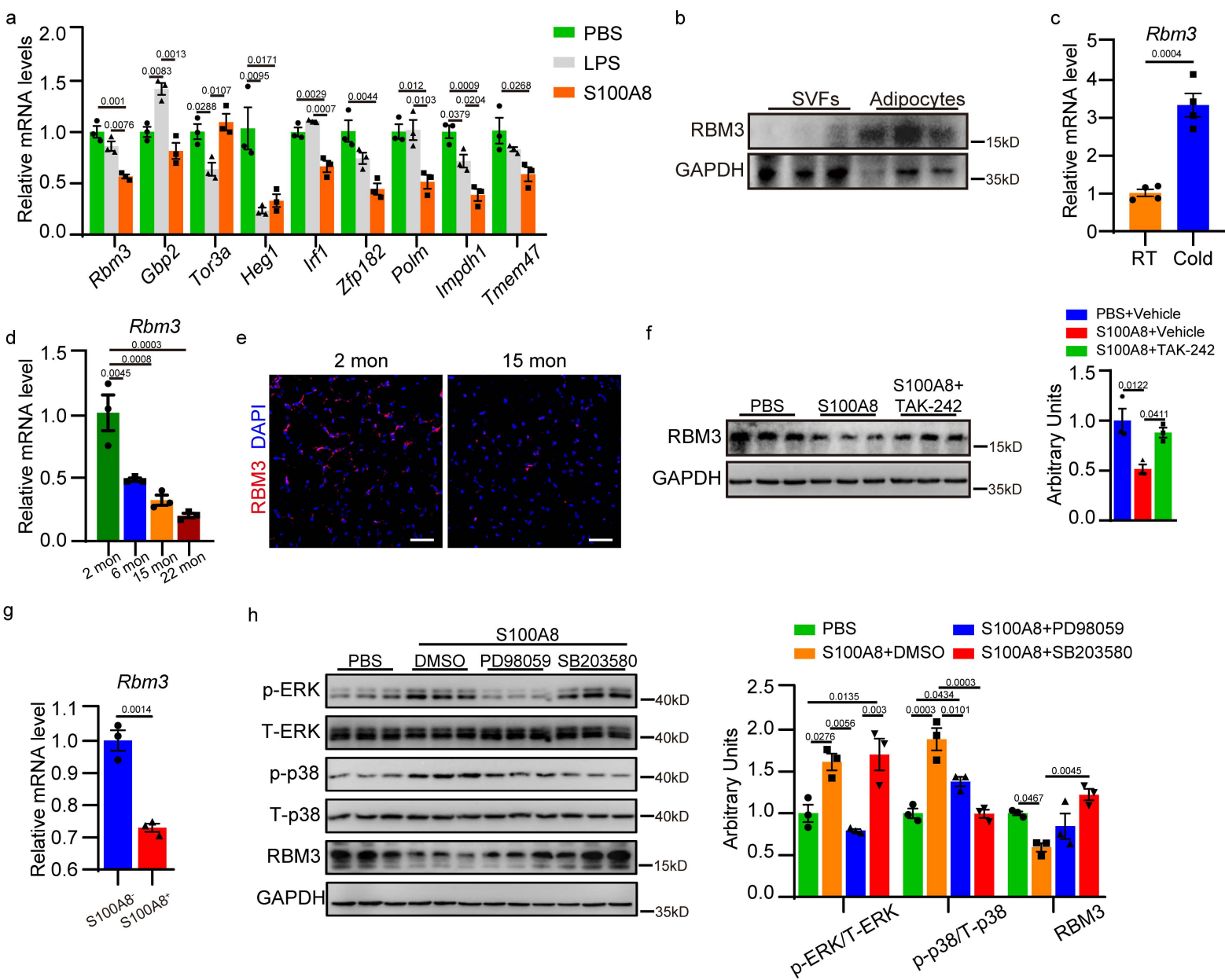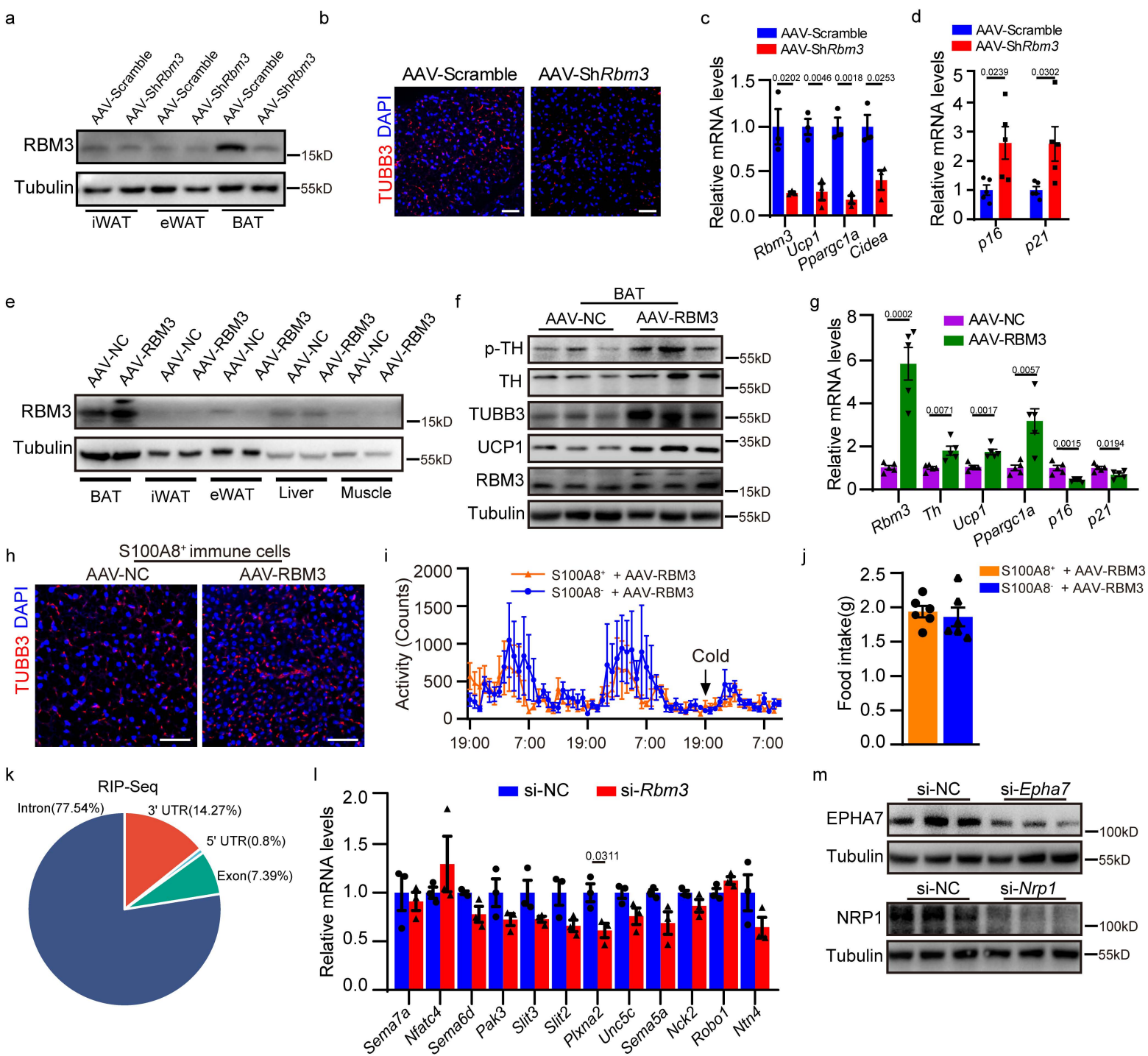
Supplementary Figure 5 RBM3 expression in the brown adipocytes is suppressed by S100A8 via TLR4-p38 axis

(a) Relative mRNA levels of S100A8 downstream candidate genes in brown adipocytes treated with PBS, LPS or S100A8 protein (n = 3).

(b) Representative immunoblots of RBM3 in SVFs and adipocytes isolated from BAT of 15-month-old mice (n = 3).

(c) Relative mRNA level of *Rbm3* in the BAT of mice subjected to cold stimulation (n = 4).

(d) Relative mRNA level of *Rbm3* in the BAT of 2-, 6-, 15- and 22-month-old mice (n = 3).

(e) Representative images of RBM3 staining in the BAT of 2- and 15-month-old mice. Scale bar, 50 μm.

(f) Representative immunoblots of RBM3 in the brown adipocytes treated

with S100A8 with or without TAK-242 (n = 3).

(g) Relative mRNA level of *Rbm3* in the BAT of mice transferred with S100A8^{+} or S100A8^{-} immune cells (n = 3).

(h) Representative immunoblots of protein / phosphorylation as indicated in

brown adipocyte treated with S100A8 in the presence of ERK1/2 inhibitor PD98059 or p38 inhibitor SB203580 (n = 3).

Data shown are representative of three independent experiments with similar results.　(n) indicates the number of biologically independent samples examined. Data are shown as the mean ± SEM. *, $P < 0.05$, **, $P < 0.01$, ***, $P < 0.001$. Statistical analysis was performed by one-way ANOVA with Bonferroni's multiple-comparisons test (a, d, f, h), or unpaired two-tailed Student's *t*-test (c, g). Statistical differences were supposed to be significant when p ＜ 0.05. Source data are provided as a Source Data File.

Supplementary Figure 6

Supplementary Figure 6 Adipose RBM3 is critical for BAT thermogenic function

(a) Representative immunoblots showing BAT-specific knockdown of *Rbm3* expression.

(b) Representative images of TUBB3 staining in BAT of mice injected with AAV-Sh*Rbm3* or AAV-Scramble. Scale bar, 50 μm.

(c) Relative mRNA levels of *Rbm3*, *Ucp1*, *Prdm16*, and *Cidea* in the BAT of mice injected with AAV-Sh*Rbm3* or AAV-Scramble (n = 3).

(d) Relative mRNA levels of *p21* and *p16* in the BAT of mice injected with AAV-Sh*Rbm3* or AAV-Scramble (n = 5).

(e) Representative immunoblots showing BAT-specific overexpression of *Rbm3*.

(f) Representative immunoblots of UCP1, TH, p-TH, TUBB3 and RBM3 in the BAT of mice injected with AAV-NC or AAV-RBM3 (n = 3).

(g) Relative mRNA levels of *Rbm3*, *Th*, *Ucp1*, *Ppargc1a*, *p16*, and *p21* in the BAT of mice injected with AAV-NC or AAV-RBM3 (n = 5).

(h) Representative images of TUBB3 staining in BAT of mice injected with AAV-NC or AAV-RBM3 and transferred with S100A8$^+$ immune cells. Scale bar, 50 μm.

(i) Activity of mice injected with AAV-RBM3 or AAV-NC and transferred with S100A8$^+$ immune cells (n = 6).

(j) Daily food intake of mice injected with AAV-RBM3 or AAV-NC and transferred with S100A8$^+$ immune cells (n = 6).

(k) Genomic distribution of RBM3 RNA immunoprecipitation sequencing (RIP-seq) peaks.

(l) Relative mRNA levels of axon guidance related genes in differentiated brown adipocytes transfected with si-*Rbm3* or si-NC (n = 3).

(m) Representative immunoblots of EPHA7 and NRP1 in brown adipocytes transfected with si-NC, si-*Epha7* or si-*Nrp1* (n = 3).

Data shown are representative of three independent experiments with similar results.　(n) indicates the number of biologically independent samples examined. Data are shown as the mean ± SEM. Statistical analysis was performed by unpaired two-tailed Student's *t*-test (c, d, g, j, i). Statistical differences were supposed to be significant when p ＜ 0.05. Source data are provided as a Source Data File.

Supplementary Table 1 Primer sequences used for real time PCR

Gene	Primer	Sequence
Mouse *Actb*	Forward primer	GATCATTGCTCCTCCTGAGC
	Reverse primer	ACTCCTGCTTGCTGATCCAC
Mouse *Rbm3*	Forward primer	CTTCGTAGGAGGGCTCAACTT
	Reverse primer	CTCCCGGTCCTTGACAACAAC
Mouse *Ppargc1a*	Forward primer	TATGGAGTGACATAGAGTGTGCT
	Reverse primer	CCACTTCAATCCACCCAGAAAG
Mouse *Ucp1*	Forward primer	AGGCTTCCAGTACCATTAGGT
	Reverse primer	CTGAGTGAGGCAAAGCTGATTT
Mouse *Cidea*	Forward primer	TGACATTCATGGGATTGCAGAC
	Reverse primer	GGCCAGTTGTGATGACTAAGAC
Mouse *Th*	Forward primer	CCAAGGTTCATTGGACGGC
	Reverse primer	CTCTCCTCGAATACCACAGCC
Mouse *p16*	Forward primer	TTGCCCATCATCATCACCT
	Reverse primer	GGGTTTTCTTGGTGAAGTTCG
Mouse *p21*	Forward primer	GCAGATCCACAGCGATATCC
	Reverse primer	CAACTGCTCACTGTCCACGG
Mouse *Tlr4*	Forward primer	ATGGCATGGCTTACACCACC
	Reverse primer	GAGGCCAATTTTGTCTCCACA
Mouse *Tnf*	Forward primer	CCCTCACACTCAGATCATCTTCT
	Reverse primer	GCTACGACGTGGGCTACAG
Mouse *Il1b*	Forward primer	GCAACTGTTCCTGAACTCAACT
	Reverse primer	ATCTTTTGGGGTCCGTCAACT
Mouse *Il6*	Forward primer	TAGTCCTTCCTACCCCAATTTCC
	Reverse primer	TTGGTCCTTAGCCACTCCTTC
Mouse *Ifng*	Forward primer	ATGAACGCTACACACTGCATC
	Reverse primer	CCATCCTTTTGCCAGTTCCTC
Mouse *Ccl5*	Forward primer	GCTGCTTTGCCTACCTCTCC
	Reverse primer	TCGAGTGACAAACACGACTGC
Mouse *Gbp2*	Forward primer	GCCAAGCTCTCTCCATCACA
	Reverse primer	AAACGTATGGCTGGGCATGA
Mouse *Heg1*	Forward primer	CGGCCTTGGAGAGCCTTC
	Reverse primer	GGAGGAGGGTGACTCTGACT

Mouse *Tor3a*	Forward primer	TACTGCCATGTGAGGCTGTG
	Reverse primer	TGGCAGATGGCTGTCTCTTG
Mouse *Impdh1*	Forward primer	TGCACGGCCTACACTCTTAC
	Reverse primer	GGAGGGAGGCTGTTCCTAGA
Mouse *Tmem47*	Forward primer	GAGCAGCGCACACTAACCTA
	Reverse primer	GCACACTCAAGCATCACTGG
Mouse *Zfp182*	Forward primer	CAGCTAGTTGGTCCGATGCG
	Reverse primer	TTCCTGCTTTTCACTCAGCTCG
Mouse *Polm*	Forward primer	TCCTCGGGCGTTATTTGCAT
	Reverse primer	ACTCTGGAAGCACAGGAAGC
Mouse *Irf1*	Forward primer	GCATTGACATGCGTCGATCA
	Reverse primer	CCCTTCCGTGGCAAATGAGTA
Mouse *Nfatc4*	Forward primer	GAGCTGGAATTTAAGCTGGTGT
	Reverse primer	CATGGAGGGGTATCCTCTGAG
Mouse *Nck2*	Forward primer	GTCATAGCCAAGTGGGACTACA
	Reverse primer	GCACGTAGCCTGTCCTGTT
Mouse *Ntn4*	Forward primer	GCAGGCTTGAATGGAGTAGC
	Reverse primer	GCAGCGTTGCATTTATCACAC
Mouse *Pak3*	Forward primer	CTGAGGATGAACAGTAACAACCG
	Reverse primer	CTGGGAAGATAGAGCGAAGCC
Mouse *Plxna2*	Forward primer	GTGCTTACACTCACCAACAATGT
	Reverse primer	AGAGCGCACAATCACACCA
Mouse *Robo1*	Forward primer	GAGCCTGCTCACTTTTACCTC
	Reverse primer	GGTCTGAAGGGTGTTCAACAAT
Mouse *Sema5a*	Forward primer	GACTTGCTAGGCCCGAGAC
	Reverse primer	TCTTTGTAAGAGACGACAGGGT
Mouse *Sema6d*	Forward primer	CCCGTTTGATGCCCGACAA
	Reverse primer	GGAAGTGTGGTTCTTTGATCCA
Mouse *Sema7a*	Forward primer	CACCGTGCTTTTCCATGAGC
	Reverse primer	CGGGGAAGTTGAAGTGGTAGAC
Mouse *Slit2*	Forward primer	AGCACCATCGAGAGGGGAG
	Reverse primer	GATCAAGCCGGTAGAGCTTCG
Mouse *Slit3*	Forward primer	TGCCCCACCAAGTGTACCT
	Reverse primer	CGCCTCTCTCGATGATGCT

Mouse *Unc5c*	Forward primer	CTGCGGACTGGGACTAGGATA
	Reverse primer	GGTTTCTGGGAGTTCGTGAAAA
Nrp1 3´UTR	Forward primer	TGTAAGCTCGGAAGGGCATC
	Reverse primer	TCCACCACAGGGTAAGGAGA
Epha7 3´UTR	Forward primer	TCGTCTGAAGATGCTGGTGA
	Reverse primer	TTGATGTGCTCGGATTGGGT